Automatic Update and Completion of Occluded Regions for Accurate 3D Urban Cartography by combining Multiple Views and Multiple Passages

Ahmad Kamal Aijazi, Paul Checchin and Laurent Trassoudaine
Clermont Université, Université Blaise Pascal, UMR 6602, CNRS, 63177 Aubiere, France

Keywords: 3D Cartography, Lidar Data, Occlusions, Multiple Views, Multiple Passages.

Abstract: Handling occlusions is one of the more difficult challenges faced today in urban landscape analysis and cartography. In this paper, we successfully address this problem by using a new method in which multiple views and multiple sessions or passages are used to complete occluded regions in a 3D cartographic map. Two 3D point clouds, from different viewing angles, obtained in each passage are first classified into two main object classes: Permanent and Temporary (which contains both Temporarily static and Mobile objects) using inference based on basic reasoning. All these Temporary objects, considered as occluding objects, are removed from the scene leaving behind two perforated 3D point clouds of the cartography. These two perforated point clouds from the same passage are then combined together to fill in some of the holes and form a unified perforated 3D point cloud of the cartography. This unified perforated 3D point cloud is then updated by similar subsequent perforated point clouds, obtained on different days and hours of the day, filling in the remaining holes and completing the missing features/regions of the urban cartography. This automatic method ensures that the resulting 3D point cloud of the cartography is most accurate containing only the exact and actual permanent features/regions. Special update and reset functions are added to increase the robustness of the method. The method is evaluated on a standard data set to demonstrate its efficacy and prowess.

1 INTRODUCTION

In the recent past, 3D urban reconstruction and Visualisation of cities have become a hot topic of research in the scientific community. Several geographical navigators like Google Streetmap Viewer, Microsoft Visual Earth or Geoportail provide real-like representation of the terrain and ground based models, created by mobile terrestrial image acquisition techniques. However, in urban environments the quality of data acquired by these hybrid terrestrial vehicles is widely hampered by the presence of temporary stationary and dynamic objects (pedestrians, cars, etc) in the scene. As a result there is a problem of occlusion of regions. Moving objects or certain temporary stationed objects (parked cars, traffic, pedestrian etc) present in the area hide certain zones of the urban landscape (buildings, road sides etc.). This paper presents a new method for handling occlusions and moreover automatic update and completion of occluded regions for accurate 3D urban cartography exploiting the concept of multiple views and multiple passages.

In order to solve the problem of occlusions, different techniques have been employed building on the advances made in the work on texture synthesis. A technique of inpainting based on the patch exemplar-based technique was presented by (Criminisi et al., 2004). This approach was extended by (Wang et al., 2008) to also infer depth from stereo pairs. A similar method was used by (Engels et al., 2011) for 3D data, but occlusions were found automatically using object-specific detectors making it more suitable for larger data sets. In the context of building facades and urban reconstruction, increased contextual knowledge is available by assuming structure's planarity and repetition of features such as floors, windows, etc. Building models are reconstructed by detecting floors and estimating building height in the work of (Konushin and Vezhnevets, 2007). Occlusions are removed by cloning upper floors and propagating them downward. A method relying on LIDAR point cloud to find and remove occlusions by combining image fusion and inpainting is presented by (Benitez et al., 2010). (Xiao et al., 2009) semantically segment street-side scenes into several classes, including vegetation and vehicles, but do not actively fill in missing data. Instead, they rely on the missing

Kamal Aijazi A., Checchin P. and Trassoudaine L. (2013).
Automatic Update and Completion of Occluded Regions for Accurate 3D Urban Cartography by combining Multiple Views and Multiple Passages.
In *Proceedings of the 2nd International Conference on Pattern Recognition Applications and Methods*, pages 405-412
DOI: 10.5220/0004182704050412

information being available from other views.

A method of aligning multiple scans from various viewpoints to ensure the 3D scene model completeness for complex and unstructured underground environments is discussed by (Craciun et al., 2010). A technique for extracting features from urban buildings by fusing camera and lidar data is presented by (Becker and Haala, 2007) but it also fails to address this problem. (Frueh et al., 2004) proposed a method in which the point cloud is used to generate a 3D mesh that is then classified as foreground or background. Large holes in the background layer, caused by occlusions from foreground layer objects, are then filled by planner or horizontal interpolation. However, such an approach may result in false features in case of insufficient repetitions or lack of symmetry (Li et al., 2011). In our work, we aim to resolve this problem by using a new approach combining both multiple views and multiple passages such that first multiple views are exploited to fill in some of the holes in the 3D point cloud followed by the use of multiple scans of the same environment obtained at different days and hours of the day to fill in the remaining holes and completing the missing regions of the urban cartography. This ensures that the resulting 3D point cloud of the cartography is most accurate containing only the exact and actual permanent features/regions. An overview of the method is presented in Algorithm 1.

2 3D SCAN REGISTRATION

Different features and robust landmarks extracted from 3D images as points of interest and as references for image mapping and scan registration have commonly been used for different multi-sessional SLAM (Simultaneous Localisation And Mapping) algorithms. This approach works well in simple repetitive paths. But some more complex situations can be found in urban environments where the selected features/regions can be occluded. When the data acquiring vehicle enters from different directions, then the path is not repetitive. As a result, the selected features/regions may not be readily visible, etc. Thus, in order to cater for this problem, the method of direct geo-referencing of 3D LiDAR points is found most suitable in our case. The method uses integrated GPS/IMU data to directly orient laser data from its local reference frame to the mapping reference frame (WGS84).The advantage of using this method is that the transformation between the local laser reference frame and the mapping reference frame is known at any given moment (as long as the laser is synchronized), independently if the laser is collecting data in a static mode or in kinematic mode. Thus, the laser can be used as a pushbroom sensor sweeping the scene with profiles while fixing the scan angles as the vehicle moves.

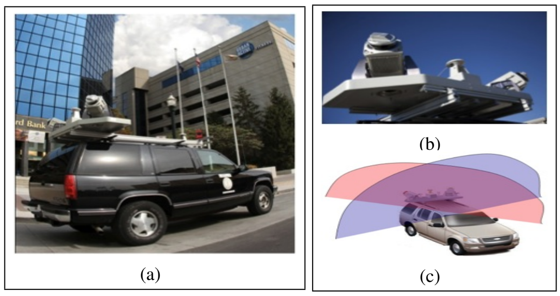

Figure 1: (a) The Vis Center's LiDAR Truck. (b) Optech LiDAR/GPS system along with IMU mounted on a rigid frame. (c) The different viewing angles of the mounted LiDAR systems.

The data that we have used to evaluate our work are the dynamic data set of the 3D Urban Data Challenge 2011, which contains dynamic scenes from downtown Lexington, Kentucky, USA obtained from the Vis Center's (University of Kentucky) LiDAR Truck containing two Optech LiDAR sensor heads (high scan frequency up to 200 Hz), a GPS, an inertial measurement unit and a spherical digital camera as shown in Figure 1.

3 CLASSIFICATION OF 3D URBAN ENVIRONMENT

We classify the urban environment into 2 main categories: Permanent objects and Temporary objects. In order to achieve this, the 3D point cloud is first segmented into objects which are then classified into basic object classes. Once classified into these basic classes, they are then grouped under one of the 2 mentioned categories. Although several methods have been proposed for the classification of urban environments, we have used one of the most recent methods (Aijazi et al., 2012) for this task. This method presents a super-voxel based approach in which the 3D urban point cloud is first segmented into voxels and then converted into super-voxels. These are then clustered together using an efficient Link-Chain method to form objects. These objects are then classified using local descriptors and geometrical features into 6 main classes: {Road, Building, Car, Pole, Tree, Unclassified}. The salient features of this method are data reduction, efficiency and simplicity of approach.

The 3D point cloud obtained from each of the two mounted LiDAR sensors is divided into the 6 object

Algorithm 1: Proposed method.

Input: 3D urban point clouds for passage number n_p
1: Classify 3D urban point cloud obtained from each of the two sensors into 6 groups: {Road, Building, Car, Pole, Tree, Unclassified}
2: Further classify the objects as: {Permanent, Temporary }
3: Separate out Temporary objects leaving behind two perforated 3D point clouds
4: Combine the two 3D point clouds of the two sensors (different viewing angles) to fill in some of the holes and obtain a unified perforated 3D point cloud $\mathbf{P}(n_p)$
5: Store Temporary objects in a register $\mathbf{R}(n_p)$
6: Match and compare $\mathbf{P}(n_p)$ with $\mathbf{P}(n_p-1)$ to fill in the remaining holes and complete 3D cartography
Update:
7: Compare Temporary objects in $\mathbf{R}(n_p)$ with $\mathbf{R}(n_p-1)$
8: Upgrade Temporary objects in $\mathbf{R}(n_p)$ if they are repeated in n_{update} number of passages as Permanent and add in $\mathbf{P}(n_p)$
Reset:
9: Compare the skyline in $\mathbf{P}(n_p)$ with that of $\mathbf{P}(n_p-1)$ to calculate 3D error difference
10: If same error difference re-occurs in n_{reset} number of passages then Reset the modified part of the building in $\mathbf{P}(n_p)$ with that in the recently acquired point cloud (perforated)
11: Update and Store $\mathbf{R}(n_p)$
12: Store point cloud $\mathbf{P}(n_p)$
13: $\mathbf{R}(n_p-1) \leftarrow \mathbf{R}(n_p)$ and $\mathbf{P}(n_p-1) \leftarrow \mathbf{P}(n_p)$
14: **return** $\mathbf{P}(n_p)$

classes using this method. These classified objects are then further classified using inference based on their basic characteristics (like roads, buildings, trees and poles cannot move whereas cars and pedestrians can be either Temporarily static or Mobile) into two classes: { Permanent , Temporary}. The classification chart as per our inference is presented in Table 1.

Table 1: Object classification chart.

Object type	Permanent	Temporary (Static or Mobile)
Road	x	
Building	x	
Tree	x	
Pole	x	
Car		x
Pedestrian		x
Unclassified		x

Once the objects present in the urban scene are classified into these two main classes, in each passage, the objects classified as Temporary are separated from the scene (for each lidar) for each passage to obtain perforated point clouds. This perforation is due to occlusions caused by the temporarily static and mobile objects in the scene. These two perforated point clouds (from different viewing angles) are merged together to form a unified 3D point cloud filling in some of the holes in the process.These unified perforated 3D point clouds of the same place obtained via a single passage on different days and at different times are then combined together to complete the 3D cartography as discussed in the following sections.

As the nature of the unclassified objects is not known, they are considered temporary by default because all the objects classified as temporary are compared in update phase. If the same objects belonging to this class are found in repeated passages, they are then upgraded as Permanent objects in the update phase discussed in Section 5.2 and are considered part of the 3D cartography.

4 COMBINING MULTIPLE VIEWS

The two 3D point clouds obtained in the same passage are matched and merged together. This not only helps in filling some of the holes but also completes the 3D cartography (building façades, etc.) due to the different viewing angles of the two sensors (from now on referred to as $\mathsf{S}-01$ and $\mathsf{S}-02$) as shown in Figure 1(c). This configuration of the LiDAR sensors is very common for this type of sensors and is used for acquiring detailed 3D data along both sides of the road. We see that this configuration of the lidar sensors not only fill in holes due to static objects present in the scene (see Figure 5) but also those caused by the mobile objects as due to this difference in viewing angle these sensors see the same point in the 3D scene with a slight time difference. This time difference allows a moving object to move such that the occluded portion of the cartography due to this object in $\mathsf{S}-01$ becomes evident in $\mathsf{S}-02$ while the occluded portion in $\mathsf{S}-02$ was evident in $\mathsf{S}-01$. Thus, combining the two 3D point clouds help fill up such holes in an attempt to eliminate the effect of the moving object in the scene as shown in Figure 5.

The two 3D point clouds are matched and merged together using the new matching method introduced in Section 5.1 to form a unified perforated 3D point cloud. This method of fusing multiple view data to fill in holes may be effective in simple cases but in more complex scenarios offered in the urban environment relying on multiple views alone does not entirely solve the problem of occlusions and a number of holes remain due to several blind spots as shown in Figure 5 (neighborhood-2). In Figure 5(c) (classic case of occlusion caused by a temporary static object, i.e. a parked car, present in the scene) it can be seen that even after combining the data from multiple views, some regions of the cartography remain occluded such as parts of shop's wall, lamppost, tree and road side.

Similarly for a temporary dynamic object, i.e. a moving car present in the urban scene, combining the data from multiple views does not fully complete all the occluded regions as seen in Figure 5(f) (some parts of shop's wall and road side remain occluded). So, this technique of combining multiple views is helpful for completion of certain occluded regions but does not solve the problem completely. Thus, in order to complete the remaining exact and actual occluded regions we use a new method exploiting the concept of multiple passages described in the next section.

5 EXPLOITING MULTIPLE PASSAGES

The unified perforated 3D point clouds obtained for each passage of any particular place are combined together to fill in the remaining holes and complete the 3D urban cartography. These 3D point clouds are first registered and then the 3D points are matched point by point, completing the missing regions.

5.1 3D Urban Point Cloud Matching

Each subsequent 3D point cloud is registered with the former point cloud by using the ICP method (Besl and McKay, 1992). This method is most suitable for this task as the 3D data are already geo-referenced and hence lie in close proximity. It is observed that the major part of the 3D urban point clouds is composed of building points which are also found to be most consistent. Thus instead of applying the ICP method to complete 3D point clouds, only the building points are taken into account. First the profile/envelope of the buildings is extracted and then the ICP method is applied, matching these boundaries to obtain the transformation matrix. The outlines/envelopes of the buildings are extracted using a sweep scan method.

As the bottom part of the building outline close to the ground is often occluded and hence inconsistent due to the presence of different objects in the scene, only the boundary of the top half of the building outline is subjected to ICP as shown in Figure 2.

Once the transformation matrix (rotation matrix $\mathbf{R}_m$ and translation matrix $\mathbf{T}_m$) is found, the whole 3D point cloud $\mathbf{P}(n_p)$ is transformed into $\mathbf{P}'(n_p)$ and then registered with the former $\mathbf{P}(n_p-1)$ using (1).

$$\mathbf{P}'(n_p) = \mathbf{R}_m(\mathbf{P}(n_p)) + \mathbf{T}_m \tag{1}$$

In order to avoid redundant points a union of 3D points belonging to the two registered point clouds

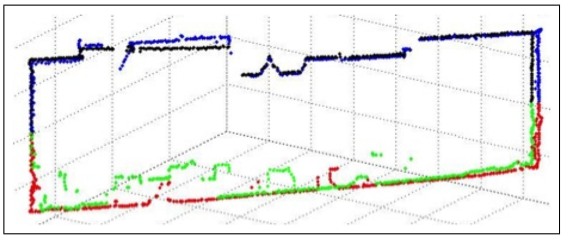

Figure 2: In red and blue color we have the building outline obtained from first passage. In green and black we have the building outline obtained from the second passage. Only top half of the two outlines in blue and black respectively is subjected to ICP.

is performed. Each 3D point of the first cloud is matched with that of the second cloud. Two corresponding points match if (2) is satisfied:

$$|\mathbf{p}_{\mathtt{Oa}} - \mathbf{p}_{\mathtt{Ob}}| \leq \sqrt[3]{\mathbf{e}_{\mathrm{tol}}} \tag{2}$$

where $\mathbf{p}_{\mathtt{Oa}}$ and $\mathbf{p}_{\mathtt{Ob}}$ (3×1 vectors) are point positions in the two point clouds along X, Y and Z axes. $\mathbf{e}_{\mathrm{tol}}$ (3×1 vector) is equal to the inverse of the maximum number of 3D points per cubic meter that is desired in the 3D cartographic map. The matched 3D points are considered as one point. This ensures that only the missing points are added completing the perforated 3D point cloud.

5.2 Update Phase

With every new passage, where the urban cartography is completed, the objects classified in each passage as Temporary are analyzed. If the same objects belonging to this class are found at the same place in repeated passages, they are then upgraded as Permanent objects and are considered part of the 3D cartography (see Algorithm 1). They are then added to the 3D cartography. Otherwise non-repetitive objects are deleted from the update register $\mathbf{R}(n_p)$. This number of allowable repetitions n_{update} can be fixed, based upon the frequency of repetition, time of repetition, etc. This not only allows gradual update of the 3D cartography but also accommodates unclassified objects in the scene; for example, in case of neighborhood-1 (see Figure 7), a few unclassified dustbins/trashcans were added to the cartography, after repetition in the successive passages, during update phase.

The Temporary objects in each passage are compared with the objects present in the update register $\mathbf{R}$ using the equations (3), (4) & (5). Simple matching based on constituting points, color and intensity is enough. Let $\mathtt{P}_{\mathtt{Obj}_n}$ and $\mathtt{Q}_{\mathtt{Obj}_n}$ be the two set of points belonging to an object n in the update register $\mathbf{R}$ and the new passage respectively. This $\mathtt{Obj}_n$ is considered to be repeated if only, and only if, the following three conditions are satisfied:

$$\frac{\mathrm{Card}(\mathtt{PQ}_{\mathtt{Obj}_n})}{\mathrm{Card}(\min[\mathtt{P}_{\mathtt{Obj}_n}, \mathtt{Q}_{\mathtt{Obj}_n}])} \times 100 \geq w_p \tag{3}$$

$$|\mathtt{P}_{\mathtt{Obj}_{nR,G,B}} - \mathtt{Q}_{\mathtt{Obj}_{nR,G,B}}| \leq 3\sqrt{w_c} \tag{4}$$

$$|\mathtt{P}_{\mathtt{Obj}_{nI}} - \mathtt{Q}_{\mathtt{Obj}_{nI}}| \leq 3\sqrt{w_I} \tag{5}$$

where $\mathtt{PQ}_{\mathtt{Obj}_n} = \mathtt{P}_{\mathtt{Obj}_{nX,Y,Z}} \cap \mathtt{Q}_{\mathtt{Obj}_{nX,Y,Z}}$. $\mathtt{PQ}_{\mathtt{Obj}_n}$ is the set containing the matched points obtained by point wise intersection of the 3D points in the two sets if, and only if, the difference in the distance along X, Y & Z axes between two points in the $\mathtt{P}_{\mathtt{Obj}_{nX,Y,Z}}$ and $\mathtt{Q}_{\mathtt{Obj}_{nX,Y,Z}}$ is $\leq 2 \times P_e$.

Here P_e is taken as the measurement accuracy of the LiDAR sensor (value can be obtained from data sheet) and Card is the cardinal number function. $\mathtt{P}_{\mathtt{Obj}_{nX,Y,Z}}$ and $\mathtt{Q}_{\mathtt{Obj}_{nX,Y,Z}}$ are the sets of the 3D coordinates of the points of the object while $\mathtt{P}_{\mathtt{Obj}_{nR,G,B}}$ and $\mathtt{Q}_{\mathtt{Obj}_{nR,G,B}}$ are the mean R,G & B values of the object in P and Q point clouds respectively. $\mathtt{P}_{\mathtt{Obj}_{nI}}$ and $\mathtt{Q}_{\mathtt{Obj}_{nI}}$ are the mean laser reflectance intensity values in P and Q point clouds respectively. w_p is the matching weight equal to the allowable percentage of the object points whose position matches the two point clouds. w_c is the color weight equal to the maximum variance of R,G & B values for $\mathtt{P}_{\mathtt{Obj}_n}$ and $\mathtt{Q}_{\mathtt{Obj}_n}$. w_I is the intensity weight equal to the maximum variance of intensity values for $\mathtt{P}_{\mathtt{Obj}_n}$ and $\mathtt{Q}_{\mathtt{Obj}_n}$.

5.3 Reset Phase

In case of a building or some part of a building is demolished in the 3D cartography due to renovation or reconstruction then the 3D point cloud is reset with the most recently acquired point cloud (perforated). In such a case, it is assumed that the removal of complete building or part of it causes a change in the skyline (or top part of the profile). This change is detected by comparing the skyline in the most recently acquired point cloud with that of the former. The 3D error difference of the two skylines is analyzed as shown in Figure 4. If the same error difference ($\Delta x, \Delta y$ and Δz in length, width and height respectively are greater than pre-defined thresholds) re-occurs in subsequent n_{reset} number of passages then only the modified part of the building in the 3D point cloud is reset (column width and thickness equal to the error size along respective axis and height equal to the building height) with that in the recently acquired point cloud (perforated). The proposed reset method was verified by synthetically removing/demolishing different parts of the buildings in the 3D cartography as shown in Figure 3. In Figure 4, the skylines in the two 3D point clouds and the 3D error difference are shown.

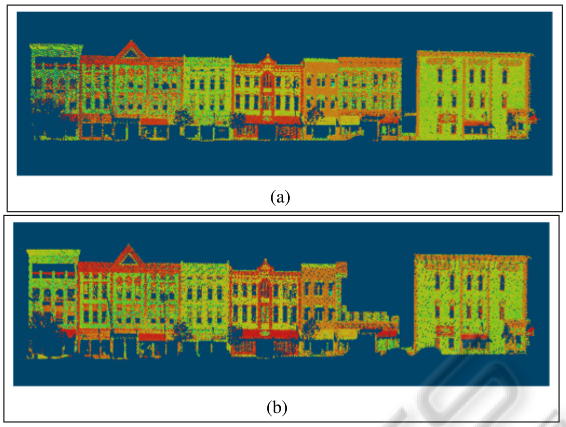

Figure 3: (a) shows the building in the first 3D point cloud. In (b) demolished building in the subsequent 3D point cloud is presented.

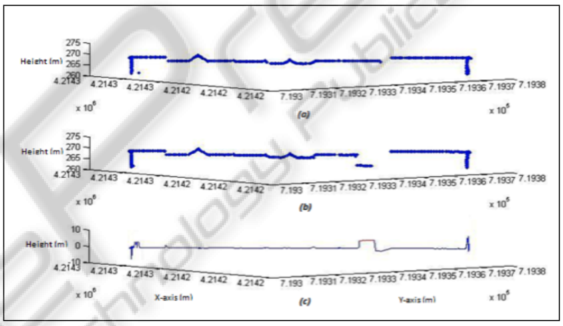

Figure 4: The skylines in the two 3D point clouds are respectively shown in (a) and (b). In (c) the 3D error of the two skylines is presented.

6 RESULTS

In order to validate our method, the dynamic data set of the 3D Urban Data Challenge 2011[1] was used. This data set contains 4 sets of the same dynamic scenes of downtown Lexington, Kentucky, USA obtained on different days and at different times. The data set consists in 3D points coupled with corresponding laser reflectance intensity values. As the corresponding RGB values are not readily available, (3) was not used. This did not have much impact on the results as laser reflectance values is found to be more consistent than RGB values in an urban environment as it is more illumination invariant (Aijazi et al., 2012). The results of our method applied to two different neighborhoods are discussed in this paper. In Figure 7, the detailed results for neighborhood-1 are presented. The value of $w_p = 75$ (i.e. if more than 75% of the object's 3D points in the two point clouds match),

[1] http://www.vis.uky.edu/3dimpvt/

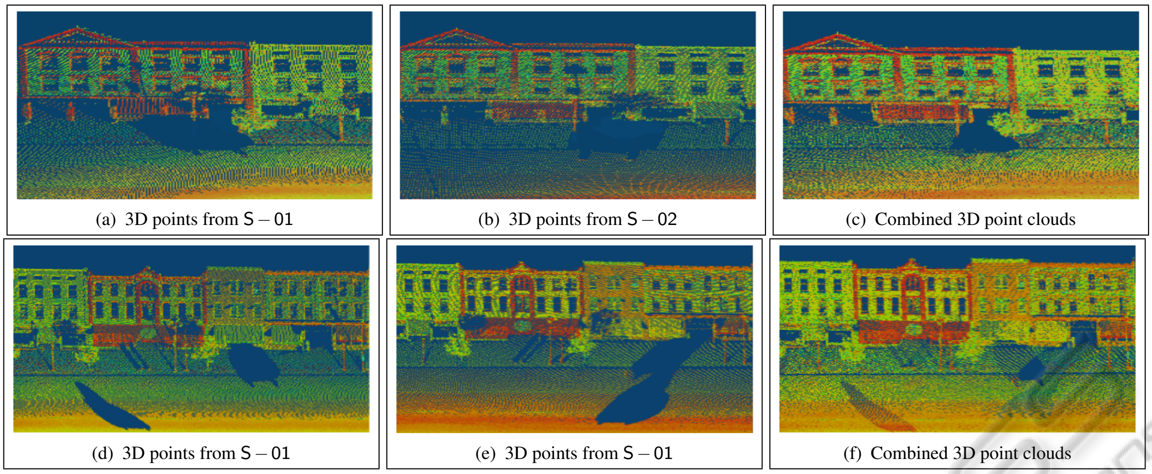

(a) 3D points from S – 01 (b) 3D points from S – 02 (c) Combined 3D point clouds

(d) 3D points from S – 01 (e) 3D points from S – 01 (f) Combined 3D point clouds

Figure 5: In (a), (b) and (c) the filling of holes due to the presence of a temporarily static (parked) car by multiple view combination is presented. In (d), (e) and (f) the filling of holes due to the presence of a temporary (dynamic) car by combining multiple views, is presented. It can be seen in (c) and (f) that even after combining data from multiple views, some holes/missing regions still remain due to blind spots.

Table 2: Classification results for permanent objects (F_1-Score).

Neighborhood	Passage 1	Passage 2	Passage 3	Passage 4	Combining multiple passages
1	0.943	0.977	0.958	0.959	0.981
2	0.979	0.975	0.981	0.984	0.992

$\mathbf{e}_{\text{tol}} = (0.000125\ 0.000125\ 0.000125)^T$ (in m^3) and $n_{\text{update}} = 4$ (maximum number of passages possible in our case) was used to evaluate our results.

6.1 Evaluation and Discussion

In order to obtain a more comprehensive analysis, firstly, the classification results were evaluated for all passages individually and then for the proposed method of multiple passages using F-measure (see (6)) as described by (Hripcsak and Rothschild, 2005).

$$F_\beta = (1+\beta^2)\frac{p.r}{(\beta^2.p+r)} \tag{6}$$

where p and r are the precision and recall respectively and β is the weight constant. The classification results of Permanent object type for neighborhood 1 and 2 are presented in Table 2. Constituting the permanent cartography, they are of most interest to us whereas all other object types are removed from the final 3D point cloud. The value of $\beta = 1$ was used to obtain a balanced F_1 score. The classified objects were considered as a percentage of their constituting points in the 3D scene. The Table 2 shows that the proposed method also improves the classification results.

Thus the proposed technique, independent of the initial classification method used, ensures that the permanent objects in the 3D urban scene are well characterized/extracted for further processing and cartography.

(a) (b)

Figure 6: (a) shows the generated 3D model of the buildings according to dimensions. In (b) one of the camera images of the building is presented.

In order to evaluate the accuracy of the completed permanent features/regions, we selected a corner building in neighborhood-1. As no ground truth was readily available, we generated the ground truth by creating a simplified 3D model of the building using a standard CAD software as shown in Figure 6. The 3D points from the initial acquisition were used for this purpose while the missing features/regions were completed by horizontal and vertical interpolation, exploiting the symmetry of the building design, and confirmed/matched with the images of the building, from different viewing angles, acquired by the digital spherical camera mounted on the vehicle (see Figure 6). A number of features/regions including the occluded zones were selected for comparison. The dimensions of these selected features updated and completed in the 3D point cloud obtained at each passage, using our method, was then compared with their corresponding dimensions in the ground truth. The average absolute errors in X, Y and Z (height) axes of the available dimensions obtained in each passage are

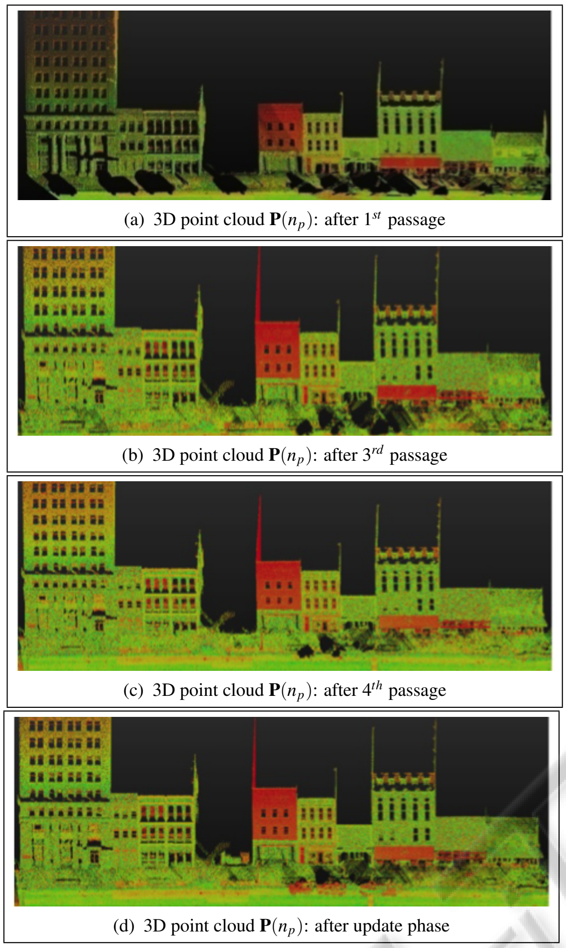

(a) 3D point cloud $\mathbf{P}(n_p)$: after 1^{st} passage

(b) 3D point cloud $\mathbf{P}(n_p)$: after 3^{rd} passage

(c) 3D point cloud $\mathbf{P}(n_p)$: after 4^{th} passage

(d) 3D point cloud $\mathbf{P}(n_p)$: after update phase

Figure 7: (a) shows the initial point cloud related to urban cartography, full of holes due to occlusions. Completion of occluded and missing regions in the urban cartography, exploiting the concept of multiple passages are presented in (b) & (c). (d) shows the updated point cloud after update phase.

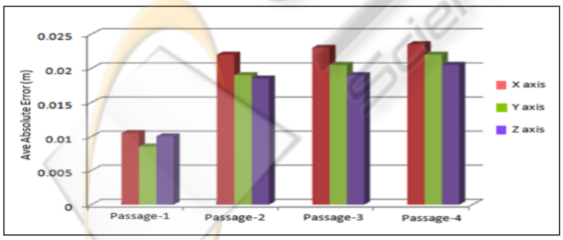

Figure 8: Average absolute errors in X, Y and Z (height) directions.

presented in Figure 8. These error values include both registration and sensor measurement errors. Low average absolute error values obtained for passage-1 are due to the fact that part of these 3D points was used for ground truth generation.

Generally, these fairly constant error values are acceptable for most applications, it is observed that the average absolute error values increase slightly in subsequent passages due to the fact that registration errors add up in every passage.

7 CONCLUSIONS

In this work, we present a new method for 3D urban cartography that successfully addresses the difficult problem concerning the automatic update and completion of occluded regions in the urban environment by combining both multiple views and multiple passages. The proposed method ensures that the resulting 3D point cloud of the cartography is most accurate that it contains only the exact and actual permanent features/regions. The evaluated results demonstrate the technical prowess of the proposed method which can be easily integrated in different commercial and non-commercial applications pertaining to urban landscape modeling and cartography that need to update their database frequently.

ACKNOWLEDGEMENTS

This work is supported by the French national research agency (ANR CONTINT iSpace&Time – ANR-10-CONT-23) and by “le Conseil Général de l’Allier”. The authors would like to thank Prof. Ruigang Yang for providing access to the 3D Urban Data Challenge data set.

REFERENCES

Aijazi, A. K., Checchin, P., and Trassoudaine, L. (2012). Classification of 3D Urban Scenes – A Voxel Based Approach. In *Int. Conf. on Pattern Recognition, Applications and Methods*, Vilamoura, Portugal.

Becker, S. and Haala, N. (2007). Combined Feature Extraction for Façade Reconstruction. In *ISPRS Workshop on Laser Scanning and SilviLaser*, page 44, Espoo, Finland.

Benitez, S., Denis, E., and Baillard, C. (2010). Automatic Production of Occlusion-Free Rectified Façade Textures using Vehicle-Based Imagery. In *Photogrammetric Computer Vision and Image Analysis*, page A:275.

Besl, P. and McKay, N. (1992). A Method for Registration of 3-D Shapes. In *IEEE Trans. on Pattern Analysis and Machine Intelligence*, volume 14(2), pages 239–256, USA.

Craciun, D., Paparoditis, N., and Schmitt, F. (2010). Multiview scans alignment for 3D spherical mosaicing in large-scale unstructured environments. *Computer Vision and Image Understanding*, 114(11):1248 – 1263.

Criminisi, A., Pérez, P., and Toyama, K. (2004). Region filling and object removal by exemplar-based inpainting. *IEEE Trans. Image Processing*, 13(9):1200–1212.

Engels, C., Tingdahl, D., Vercruysse, M., Tuytelaars, T., Sahli, H., and Van Gool, L. (2011). Automatic occlusion removal from façades for 3D urban reconstruction. *Advanced Concepts for Intellig. Vision Systems*, pages 681–692.

Frueh, C., Sammon, R., and Zakhor, A. (2004). Automated texture mapping of 3D city models with oblique aerial imagery. In *Proc. of 2nd Int. Symp. on 3D Data Processing, Visualization and Transmission (3DPVT)*, pages 396–403. IEEE.

Hripcsak, G. and Rothschild, A. S. (2005). Agreement, the F-Measure, and Reliability in Information Retrieval. *Journal of American Medical Iinformatics Association*, 12(3):296–298.

Konushin, V. and Vezhnevets, V. (2007). Automatic building texture completion. In *Proc. Graphicon'2007*, Moscow, Russia.

Li, Y., Zheng, Q., Sharf, A., Cohen-Or, D., Chen, B., and Mitra, N. J. (2011). 2D-3D Fusion for Layer Decomposition of Urban Facades. In *IEEE Int. Conf. on Computer Vision (ICCV)*, Barcelona, Spain.

Wang, L., Jin, H., Yang, R., and Gong, M. (2008). Stereoscopic inpainting: Joint color and depth completion from stereo images. In *IEEE Conf. on Computer Vision and Pattern Recognition (CVPR)*, pages 1–8.

Xiao, J., Fang, T., Zhao, P., Lhuillier, M., and Quan, L. (2009). Image-based street-side city modeling. *ACM Trans. Graph.*, 28:114:1–114:12.